

Article

A Systematic Study of the Cryogenic Milling of Chrysotile Asbestos

Valentina Scognamiglio ¹, Dario Di Giuseppe ^{1,2,*} , Magdalena Lassinantti Gualtieri ^{3,4}, Laura Tomassetti ^{1,5}  and Alessandro F. Gualtieri ¹ 

- ¹ Department of Chemical and Geological Sciences, University of Modena and Reggio Emilia, Via G. Campi 103, I-41125 Modena, Italy; vscognam@unimore.it (V.S.); laura.tomassetti@iia.cnr.it (L.T.); alessandro.gualtieri@unimore.it (A.F.G.)
- ² Department of Sciences and Methods for Engineering, University of Modena and Reggio Emilia, Via Amendola 2, I-42122 Reggio Emilia, Italy
- ³ Department of Engineering “Enzo Ferrari”, University of Modena and Reggio Emilia, Via P. Vivarelli 10/1, I-41125 Modena, Italy; magdalena.gualtieri@unimore.it
- ⁴ Interdepartmental Research Centre for Applied Research and Services in the Advanced Mechanics and Motor Sector, University of Modena and Reggio Emilia, Via Pietro Vivarelli 2, 41125 Modena, Italy
- ⁵ National Research Council of Italy, Institute of Atmospheric Pollution Research (CNR-IIA), Via Salaria 29300, I-00015 Monterotondo, Italy
- * Correspondence: dario.digiuseppe@unimore.it; Tel.: +39-059-205-8497

Abstract: For more than 40 years, intensive research has been devoted to shedding light on the mechanisms of asbestos toxicity. Given the key role of fibre length in the mechanisms of asbestos toxicity, much work has been devoted to finding suitable comminution routes to produce fibres in desired size intervals. A promising method is cryogenic milling that, unlike other mechanical size reduction techniques, preserves the crystal–chemical properties of materials. In this study, the effect of cryogenic milling on the physical–chemical properties of commercial Russian chrysotile was studied in order to produce precise size fractions with invariant properties compared to the pristine fibres. In particular, two batches with fibres $> 5 \mu\text{m}$ and $< 5 \mu\text{m}$ were prepared, as this limit sets their potential toxicity. The results are fundamental for future *in vitro* toxicity testing of this commercial product, widely used in chrysotile-friendly countries but not yet adequately studied. Results show that fibre length can be controlled by milling time under cryogenic conditions without inducing structural defects or amorphization; short fibres (95% $L < 5 \mu\text{m}$) can be obtained by cryogenic milling for 40 min, while 10 min is enough to yield long chrysotile fibres (90% $L > 5 \mu\text{m}$).

Keywords: asbestos; chrysotile; fibres length; cryogenic milling; size-selective method



Citation: Scognamiglio, V.; Di Giuseppe, D.; Lassinantti Gualtieri, M.; Tomassetti, L.; Gualtieri, A.F. A Systematic Study of the Cryogenic Milling of Chrysotile Asbestos. *Appl. Sci.* **2021**, *11*, 4826. <https://doi.org/10.3390/app11114826>

Academic Editor: Patrick A. Fairclough

Received: 29 April 2021

Accepted: 20 May 2021

Published: 25 May 2021

Publisher’s Note: MDPI stays neutral with regard to jurisdictional claims in published maps and institutional affiliations.



Copyright: © 2021 by the authors. Licensee MDPI, Basel, Switzerland. This article is an open access article distributed under the terms and conditions of the Creative Commons Attribution (CC BY) license (<https://creativecommons.org/licenses/by/4.0/>).

1. Introduction

The term asbestos refers to a group of six mineral fibres of significant industrial and economic importance that have been widely used since antiquity [1]. Members of the asbestos group are chrysotile (serpentine group), and five species of amphiboles: crocidolite (fibrous riebeckite), amosite (fibrous cummingtonite–grunerite) and the fibrous variety of anthophyllite, actinolite and tremolite [2,3]. Today, there is enough scientific evidence to state that inhalation of asbestos may induce fatal lung diseases, such as lung cancer, malignant mesothelioma (MM), and asbestosis [3,4]. Accordingly, asbestos is included by the International Agency for Research on Cancer (IARC) in Group 1 as a carcinogen for human [3]. The most insidious asbestos-related disease is undoubtedly MM [5–7]. This aggressive type of cancer originates from the pleural cavity (i.e., the serous membrane that separate the lungs and the wall of the thoracic cavity) to which asbestos fibres can reach due to their favourable aerodynamic diameter [8,9]. The carcinogenesis of MM is initiated by the inflammatory response to those fibres that are retained in the pleural cavity, being too long to exit through the stomatal openings in the parietal pleural surface (diameter

in the range 3–10 μm) and migrate to the lymphatic capillary system [5,7,8]. Hence, the toxicity potential of long fibres is higher. It should be pointed out that this is only one piece of the puzzle. The complex toxicity mechanisms, being multifactorial and related to different cell–fibre interactions, is not yet fully understood [5,10]. In addition, there is still debate as to whether or not chrysotile is less potent than amphibole asbestos in causing mesothelial carcinogen in humans. The main reason for which chrysotile is considered less hazardous than the other asbestos minerals is its lower biodurability [11]. The chrysotile fibres are, in fact, rather quickly dissolved in the intracellular macrophage environment in contrast to the amphiboles that remain in the lungs, even for a lifetime [12,13]. The pro-chrysotile community therefore sustains that asbestos-induced diseases apparently linked to chrysotile exposure are actually due to contamination by amphibole asbestos [14]. This so-called “amphibole hypothesis” is now rejected by most of the scientific community and recently published occupational epidemiology studies assert a clear correlation between chrysotile exposure and increased mortality from MM [15,16]. Nevertheless, this issue cannot be considered univocally resolved, as only a relatively few studies were aimed at evidencing the dose–response relationship for cancer following exposure to different fibre types in the same exposed population [3,17]. In this context, the technological advances in the field of *in vitro* models can provide new and effective approaches for studying asbestos toxicity. However, a confident and unequivocal protocol for making asbestos fibre samples with defined and proper textural characteristics suitable for *in vitro* testing is still lacking [18].

Following the continuous awareness of health hazards related to asbestos exposure, the exploitation of amphibole asbestos is now globally banned. However, for the reasons discussed above, controlled use of chrysotile is still allowed in ca. 66% of all countries in the world [19]. The 2019 trade data show that the extractions in the Russian Federation (750,000 t/year), Kazakhstan (200,000 t/year), China (125,000 t/year), Brazil (15,000 t/year) and Zimbabwe (2500 t/year) stand for over 99% of the total world production of chrysotile (1,100,000 t/year) (USGS, 2020). The by far most important producer is the Russian Federation that alone stands for ca. 68% of the total [20]. Extraction sites are located in the Urals Mountains. In our recent work [21], a commercial Russian chrysotile extracted by Orenburg minerals (Yasniy) was extensively characterized and found to resemble the Italian Balangero chrysotile that has caused, and continues to cause, asbestos-related diseases in the exposed population [22]. This chrysotile is currently used for a myriad of products found in everyday life (e.g., textiles, paddings, sealing materials, frictional production, cardboard, and asbestos–cement products), and claimed to be safe by the mining industry due to the lack of conclusive scientific evidence linking exposure to chrysotile with MM. Hence, the continuous exploitation of Russian chrysotile may be an important health concern that, unfortunately, today, is in the shadow of financial gain. Although much progress has been made in enlightening the mechanism by which chrysotile induces cyto- and genotoxic damage, work is still needed and surely also complicated by structural and chemical variabilities that are observed among fibres of different geological origin [21,23].

Considering the major role played by fibre length in determining the toxicological action of asbestos, controlling this parameter is of paramount importance in targeted studies. Methods need to be developed that allow the preparation of sets of fibres that only differ in size. Many more or less sophisticated routes have been suggested for chrysotile, generally involving comminution of pristine fibres followed by separation by size [23–26], although direct separation of pristine samples through sedimentation in water was also attempted [27]. However, the latter approach was shown to be rather inflexible, as only a fine fraction with controlled length was obtained ($90\% < 2 \mu\text{m}$) [27]. In fact, considering that the chrysotile fibres are very long ($>10 \mu\text{m}$), reduction in fibre length before any separation process is preferred. The choice of comminution method is of paramount importance, as the crystal–chemical properties of the fibres must not be altered. Table 1 lists the methods currently available for mechanically milling chrysotile fibres. Mechanical milling is one of the most common size reduction methods in general and has been extensively evaluated

as a potential route for the preparation of fibres with controlled lengths. Size reduction by mechanical milling occurs due to a combination of impact, compression and shear forces [28]. Both the type of equipment and experimental parameters highly influence the imposed forces and the consequent material's response. Many different types of instrumental setups have been used to systematically investigate the effect of mechanical action on chrysotile. These include dry milling in planetary ball mills [29–32], milling in vibration ball mills in dry conditions as well as in the presence of hydrocarbons or water [33–35], dry milling in a vibration disc mill [36], and rotary mill (also called ring and puck mill or shutter box) [37]. Generally speaking, size reduction was accompanied by plastic deformation of the chrysotile structure and prolonged mechanical action eventually led to complete amorphization. Hence, alternative methods have been proposed that were shown to avoid structural–chemical modifications with respect to the pristine fibres: prolonged ultrasonification [34,38], gentle hand-milling [26] and chopping [24]. A promising comminution method that leaves intact the chemical–structural properties of chrysotile is cryogenic milling [23,39], which exploits the brittle fracture of materials cooled down to cryogenic temperatures [40–42]. In the present study, the effect of cryogenic milling on the chemical–structural properties of a commercial Russian chrysotile (Orenburg minerals, Yasniy) was investigated for various milling times in order to prepare different length fractions of fibres for toxicological studies. The crystallinity, chemistry, particle size and morphology of chrysotile fibres were measured by X-ray diffraction, Fourier Transform Infra-Red spectroscopy, Scanning Electron Microscopy and Energy Dispersive X-ray.

Table 1. Comparison of different methods used for milling chrysotile.

References	Milling Methods	Environmental Conditions	Advantages/Disadvantages
[23]	Cryogenic vibro-milling with steel balls	−150 °C and wet condition	Preservation of chrysotile crystallinity
[32]	Mechanical friction with cylindrical milling elements	Room temperature and wet condition	Reduction in chrysotile crystallinity
[32]	Agate mortar	Room temperature and dry condition	Reduction in chrysotile crystallinity
[33,35]	Ball milling	Room temperature and dry condition	Reduction in chrysotile crystallinity
[34,35]	Ball milling	Room temperature and wet condition	Water-wet conditions preserves the chrysotile crystallinity
[36]	Ring mill equipped with a tungsten carbide bowl	Room temperature and dry condition	Reduction in chrysotile crystallinity
[37]	Rotary mill	Room temperature and dry condition	Reduction in chrysotile crystallinity

2. Materials and Methods

2.1. Sample Preparation and Characterisation

A commercial chrysotile sample from the Russian Federation, extracted by Orenburg Minerals from an open pit mine near the town Yasniy was used in this work. This particular sample was extensively characterised in our previous work wherefore only a short description will be given here [21]. The sample is composed of bundles of fibres up to 1 mm in length that easily split lengthwise into fine fibres and thin bundles. The length of a single fibre and thin bundles is in the range of 1.36 to 188.1 µm (mean 33.9 µm), whereas the fibre width is in the 0.05–2.79 µm range (average 0.7 µm). Clino-chrysotile is the major phase, accompanied by minor amounts of ortho-chrysotile, lizardite, magnetite, hydromagnesite and calcite. The composition, determined by electron probe microanalysis (EPMA), was [(Mg_{2.870}Fe²⁺_{0.027}Al_{0.034}Cr_{0.005}Ni_{0.006})_{2.986}(OH)₄Si_{1.92}O₅] (Fe²⁺/Fe³⁺ ratio from Mössbauer spectroscopy).

The milling experiments were conducted, using a Retsch mixer mill MM 400 (Düsseldorf, Germany), equipped with two processing stations. This is the very same equipment that was used to prepare powder batches for various analyses in our previous work dealing

with this Russian sample [21]. The milling jars (35 mL) are made of steel and each one is accompanied with a steel milling ball (diameter of 20 mm, weight 14.24 g). The lining of the jar and balls is made of polytetrafluoroethylene (PTFE), which serves to prevent contamination of the sample with metals from the jar and balls during milling. The loaded jar is submerged in liquid nitrogen until acquiring the temperature of the surrounding medium and subsequently mounted in the mixer mill. During operation, the jar oscillates from side to side with a pre-set frequency (3–30 Hz). The amplitude of the oscillations is fixed. The repeated impaction of the ball against the embrittled material leads to size reduction. In the experiments performed in our laboratory, the jars were loaded with 1 g of raw chrysotile and an oscillation frequency of 30 Hz was applied for various durations, i.e., 5, 10, 20, 30, and 40 min. The investigated range of milling durations were chosen based on preliminary tests, evidencing too-low efficiency following durations of less than 5 min and a non-significant improvement of the size reduction for duration longer than 40 min. From now on, samples will be denoted by CHR (pristine chrysotile) followed by the milling duration if processed.

2.2. Characterisation Techniques

Morphometric investigation of chrysotile fibres following various milling durations were performed, using a JSM-6010PLUS/LA Scanning Electron Microscopy (SEM) equipped with and Energy Dispersive X-ray (EDX) spectrometer (Oxford INCA-350). EDX is an analytical method useful for identify and quantify (only semi-quantitative results) the elementary compositions of the materials observed with the SEM. EDX analyses were conducted to verify the changes in the elemental composition undergone by the chrysotile fibres after prolonged milling. Specimens for these analyses were prepared as follows: some milligrams of fibres were suspended in 5 mL of ethanol and a drop of the resulting suspension was placed on conductive, double-stick carbon tape attached to an aluminium stub [43]. After complete evaporation of the solvent, the specimen was coated with a thin film of carbon (10 nm thick), using a Carbon Coater-Balzers CED-010. The length of the chrysotile fibres was determined by processing SEM images obtained by secondary electron imaging and appropriate magnifications (500–20,000×). A series of representative SEM images were analysed using ImageJ software, which provides accurate measurements of the lengths of both straight and curved fibres [44]. The fibre length distributions were constructed based on a statistically representative number of fibres (Table 2). As mentioned above, Russian chrysotile forms irregular, curvilinear aggregates of fibres and fibril bundles. Therefore, the length of the fibres was measured for each sample, considering both single fibres and fibril bundles.

Table 2. Fraction of chrysotile fibres comprised in a given interval of fibre length after each milling treatment and main statistical parameters of fibre lengths. Raw chrysotile (CHR); chrysotile after 5 min of milling (CHR5); chrysotile after 10 min of milling (CHR10); chrysotile after 20 min milling (CHR20); chrysotile after 30 min of milling (CHR30); chrysotile after 40 min of milling (CHR40). Number of fibres (N).

	CHR	CHR5	CHR10	CHR20	CHR30	CHR40
Length classes (µm)						
0–5	7.00%	9.43%	12.5%	34.4%	65.3%	95.2%
5–10	7.50%	21.7%	41.7%	32.8%	28.1%	1.08%
10–15	10.5%	11.3%	16.7%	11.5%	2.04%	1.61%
15–20	13.5%	8.49%	12.5%	6.56%	3.57%	0.54%
>20	61.5%	49.1%	16.7%	14.8%	1.02%	1.61%
Average (µm)	33.9	29.80	14.32	10.7	4.89	1.91
Maximum (µm)	188.1	159.8	79.9	53.6	22.1	22.1
Minimum (µm)	1.36	1.45	2.02	1.29	0.43	0.25
Standard error	1.99	3.08	2.08	1.34	0.27	0.21
N	200	100	100	100	200	200

X-ray powder diffraction (XRPD) data were collected using an X'Pert PRO PANalytical θ/θ diffractometer (CuK α radiation, 40 kV and 40 mA), equipped with a stripe detector (X'Celerator). Powders were mounted in aluminium sample holders, using a side-loading technique. A step scan of $0.0167^\circ 2\theta$ was used with a time of 1 s/step in the 5° – 40° 2θ range. The incident beam pathway included a $1/4^\circ$ divergence slit and $1/4^\circ$ anti-scattering slit. The pathway of the diffracted beam included a soller slit (0.04 rad), an antiscatter blade (5 mm) and a Ni filter. The XRPD patterns were analysed using the X-Pert High Score Plus software DATABASE [45].

Fourier Transform Infra-Red (FTIR) spectroscopy analyses of the chrysotile samples were performed in the spectral range 600 – 4000 cm^{-1} , using a Bruker Vertex 70 spectrometer (Ettlingen, Germany) equipped with a DTGS detector and a KBr beam splitter. The spectrometer was coupled to a horizontal attenuated total reflectance (ATR) device consisting of a diamond crystal of 2 mm in diameter (Platinum ATR-QL, Bruker Optics, Ettlingen, Germany). ATR-FTIR spectroscopy is a fast, non-destructive, non-invasive, reagent-free, sensitive, and highly reproducible physicochemical tool for characterisation of mineral fibres [46–48]. In addition, ATR-FTIR requires only a small amount of sample for analysis with easy and quick preparation [46].

3. Results

3.1. SEM Characterisation

Figure 1 shows SEM micrographs of pristine chrysotile fibres as well as fibres exposed to cryomilling for different durations. As already reported in our previous work [21], the pristine sample (CHR) is composed of very long fibre bundles (up to 1 mm in length) with split ends (Figure 1a) accompanied by clusters of intertwined fibres (Figure 1b). The fibres are very long and curly (mean $L = 33.9$ μm) (Figure 1a). The SEM images show some important morphological changes following milling (Figure 1c–f). Although most fibres are still aggregated in bundles and clusters after 5 min of milling (CHR5), the bundle length is reduced (Figure 1c). Following 10 min of milling (CHR10), short bundles are observed together with single fibres that have apparently been separated from the bundles/clusters (Figure 1d). Increasing the milling time (10 min steps) up to a total of 40 min leads to progressively shorter fibre bundles and single fibres with decreased curliness (Figure 1e–h).

From the analyses of SEM images, the fibre length distribution (i.e., the fraction of fibres comprised in a given length interval) was determined for pristine chrysotile and for chrysotile exposed to cryogenic milling for various durations. The results are shown in Figure 2 and Table 2. Length intervals were fixed to 0–5 μm , 5–10 μm , 10–15 μm , 15–20 μm , >20 μm . As shown in Figure 2, the length of the fibres decreases as a function of milling time. Pristine chrysotile (CHR) exhibits 61.5% of the fibres longer than 20 μm (Figure 2a). After 5 min of milling, this length class is reduced to a value of 49.1%, while the percentage of fibres falling within the range of 5–10 μm increases from 7.5% to 21.7% (Figure 2b). After 10 min (CHR10), approximately 50% of the fibres are shorter than 10 μm (Figure 2c). Increasing the milling time to 20 min (CHR20) further increases the percentage of this length class to 67% (Figure 2d). The most substantial size reduction is observed following 30 min of milling (Figure 2e). After 30 min, the fibres that belong to the range 0–5 μm are 65%, while the percentage of fibres longer than 20 μm is dropped to 1% (Figure 2e). Finally, after 40 min, almost all fibres (95%) are shorter than <5 μm (Figure 2f).

Since chrysotile is mainly composed of Si and Mg, the SEM-EDX semi-quantitative analyses focused on these two elements. Table 3 shows the Si and Mg content (reported in weight percentages of the oxides of the elements) of raw and ground Russian chrysotile (40 min) fibres measured by SEM-EDX. The semi-quantitative composition of the two samples is comparable. Very similar is the Si/Mg ratio, 1.05 for raw chrysotile and 1.02 for long-term milled chrysotile. Therefore, no Mg depletion was induced during cryomilling.

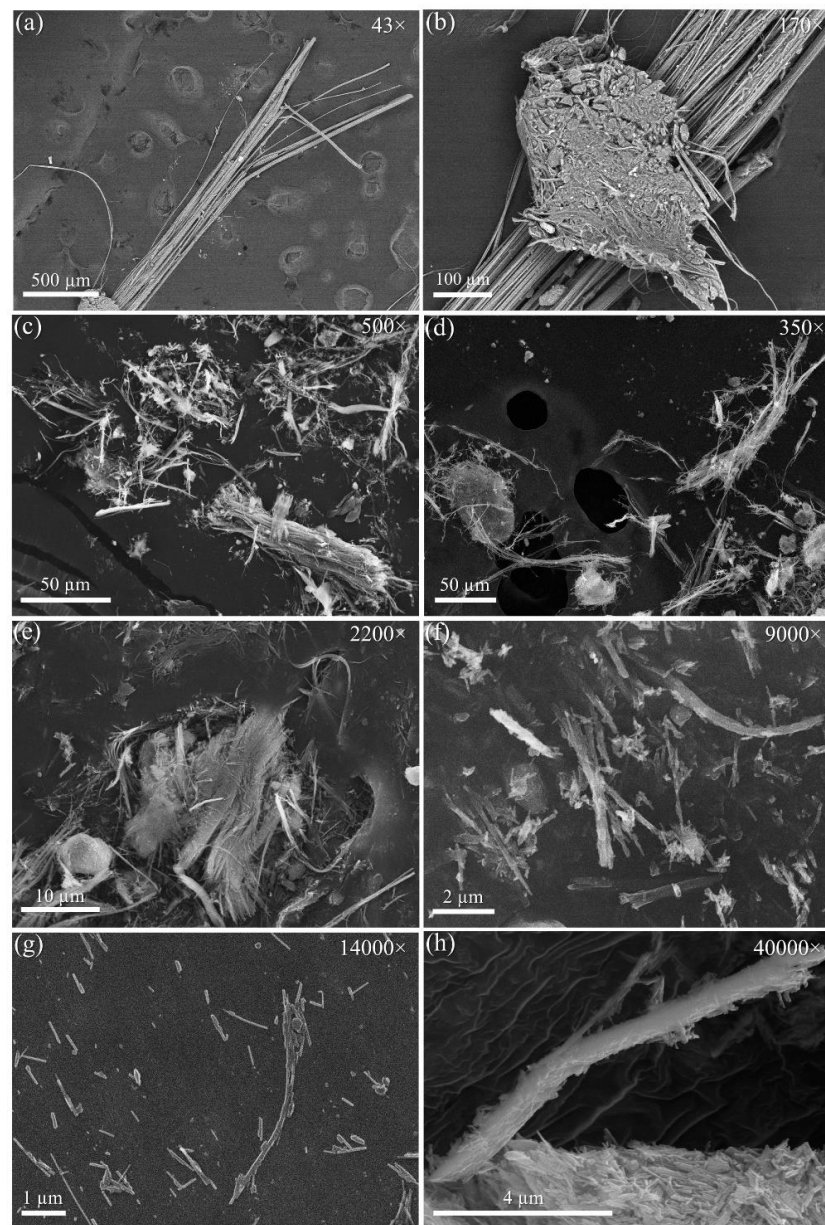


Figure 1. SEM images of Russian chrysotile. (a) An example of the long fibre bundles in raw chrysotile (CHR). (b) Detail of the bundle shown in (a) with intertwined fibres cluster. (c) Chrysotile after 5 min of milling (CHR5). (d) Chrysotile after 10 min of milling (CHR10). (e) Chrysotile after 20 min milling (CHR20); (f) Chrysotile after 30 min of milling (CHR30). (g,h) Chrysotile after 40 min of milling (CHR40).

Table 3. Si and Mg content (expressed in terms of weight percent oxides) and Si/Mg ratio of raw and ground Russian chrysotile (40 min) fibres determined by 50 SEM-EDX spot analyses. Standard error of the mean in brackets.

	Min	Max	Mean	Si/Mg
Raw chrysotile				
SiO ₂	47.79	53.61	50.58 (1.2)	1.05
MgO	42.15	50.84	48.27 (2.1)	
Chrysotile 40 min				
SiO ₂	38.74	55.39	49.46 (0.5)	1.02
MgO	40.49	61.26	48.31 (0.7)	

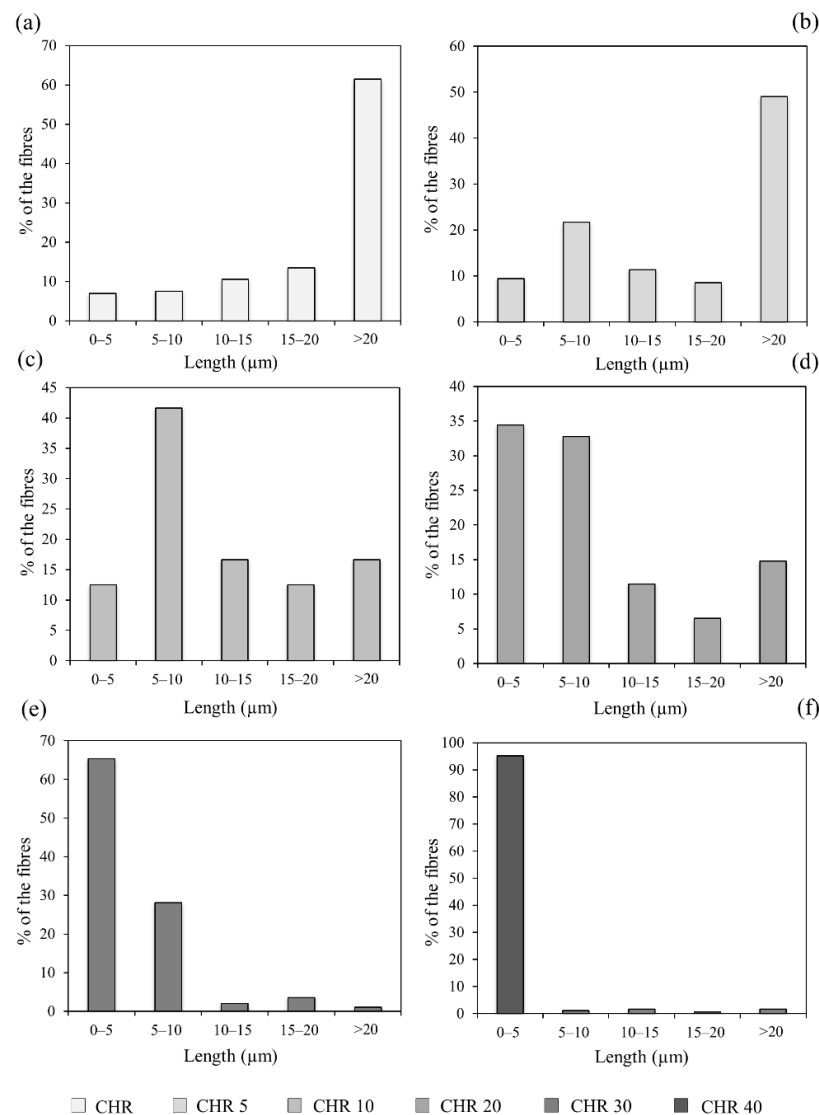


Figure 2. Chrysotile fibre length distribution (i.e., the fraction of fibres comprised in a given interval of fibre length) after each milling treatment. (a) Raw chrysotile (CHR). (b) Chrysotile after 5 min of milling (CHR5). (c) Chrysotile after 10 min of milling (CHR10). (d) Chrysotile after 20 min milling (CHR20). (e) Chrysotile after 30 min of milling (CHR30) (f) Chrysotile after 40 min of milling (CHR40).

3.2. XRPD Characterisation

Figure 3 shows the XRPD patterns collected from pristine and cryo-milled chrysotile. Qualitative mineralogical analysis of pristine chrysotile evidences the presence of clinochrysotile as major phase, accompanied by some minor phases (i.e., ortho-chrysotile, lizardite, magnetite, hydromagnesite and calcite). This result confirms the previous published data [21].

The typical anisotropic diffraction peak broadening due to a distorted unit cell originating from the cylindrical lattice is evident [23].

From Figure 3 it is clear that cryo-milling does not provoke any changes in the diffraction pattern, i.e., crystallinity and microstructure remain invariant. This is further evidenced in Figure 4 that shows the (002) reflection of chrysotile for all investigated samples (a) together with the Full Width at Half-Maximum (FWHM) as a function of milling time for the same reflection (b). In fact, both reflection intensity as well as peak breadth remain invariant.

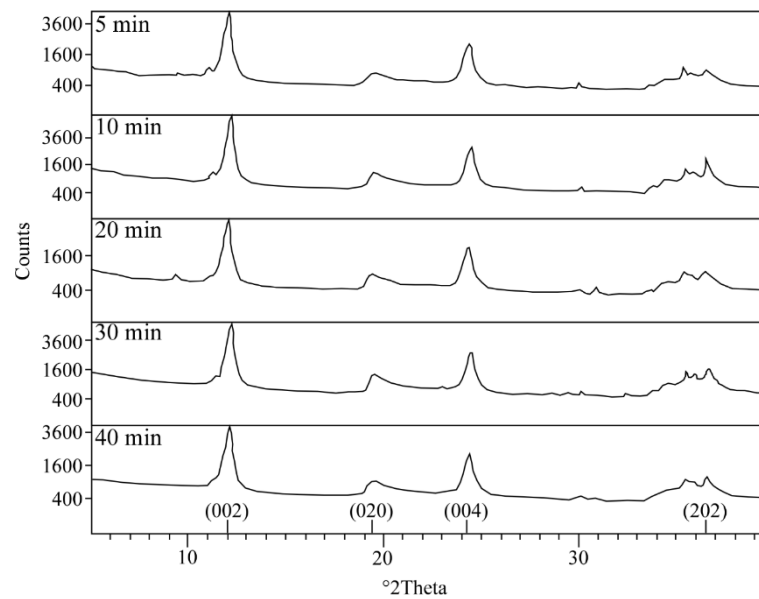


Figure 3. X-ray diffraction pattern of cryo-milled chrysotile with different time of milling. The main diagnostic peaks for chrysotile with their Miller indices are shown.

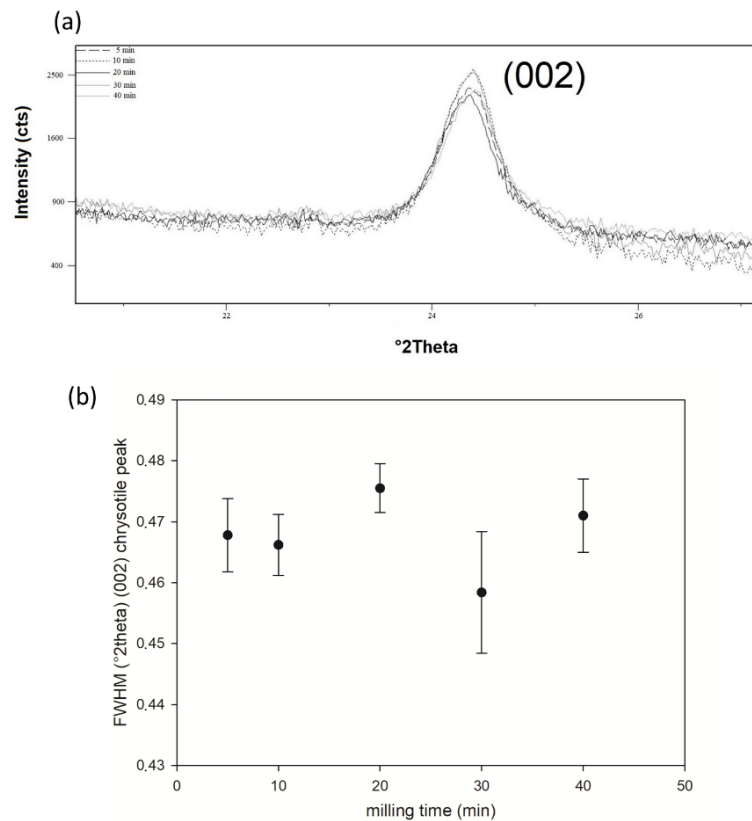


Figure 4. (a) X-ray diffraction pattern of cryo-milled chrysotile in the $^{\circ}2\text{Theta}$ range from 21 to 27. The image shows the negligible effect of milling on the chrysotile (002) peak. (b) Variation of Full Width at Half-Maximum (FWHM) of (002) chrysotile peak with time of milling.

3.3. FTIR Characterisation

The FTIR spectra of the samples are reported in Figure 5. In particular, the entire investigated spectral range is shown in Figure 5a, whereas a restricted range ($3600\text{--}3720\text{ cm}^{-1}$) is shown in Figure 5b in order to evidence the absorption peak assigned to the O–H stretching

vibrations [48]. The intense peaks at 950, 1020 and 1074 cm^{-1} are related to the Si–O bond [49]. The two peaks at 1420 and 1480 cm^{-1} can be assigned to the MO–H ($M = \text{Mg}^{2+}$ or Fe^{2+}) stretching vibrations modes [50]. The OH-stretching region 3600–3720 cm^{-1} (Figure 5b) shows two well-defined absorption bands. 3682 cm^{-1} intense band is assigned to external MO–H groups, whereas 3643 cm^{-1} medium band is assigned to internal MO–H groups [51]. The most important information retrieved from Figure 5 is that the spectra (relative absorption intensities and peak positions) collected from the samples are nearly identical (Figure 5). Only some minor differences can be observed in the absolute intensity of the bands, which is not surprising considering the difficulties in reproducing the contact area between the sample and the ATR crystal and, thus, the peak intensity [52].

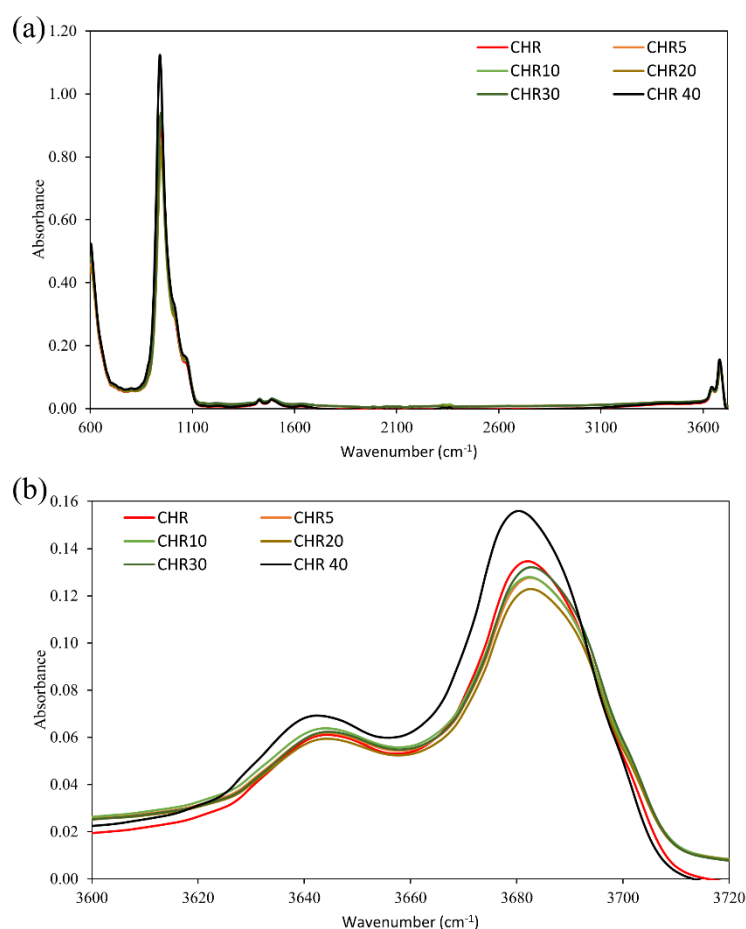


Figure 5. (a) FTIR spectra (600–4000 cm^{-1}) of raw Russian chrysotile (CHR), chrysotile after 5 min of milling (CHR5), chrysotile after 10 min of milling (CHR10), chrysotile after 20 min milling (CHR20), chrysotile after 30 min of milling (CHR30) and chrysotile after 40 min of milling (CHR40). (b) The OH-stretching region.

4. Discussion

Considering the major role played by fibre length in determining the toxicological action of asbestos, controlling this parameter is of paramount importance in targeted studies. Preparing batches of chrysotile fibres only differing in length generally involve size reduction of pristine fibres followed by separation. The first step is crucial, as alternation of the fibre properties must be avoided. The scientific literature has discarded traditional milling by way of reducing fibre length, as the mechanical action leads to plastic deformation of the chrysotile structure (Table 1).

In the present study, cryogenic milling was systematically explored as a potential size reduction technique. More precisely, the structural integrity was verified following various

milling durations, using XRPD and FTIR, which are powerful techniques in evidencing structural changes on a molecular level.

The summary graphs in Figure 6 show the percentage of long ($L > 5 \mu\text{m}$) and short ($L < 5 \mu\text{m}$) Russian chrysotile fibres as a function of milling time (0 to 40 min). According to Figure 6, increased duration of cryogenic milling resulted in a successive reduction in fibre length. The longest milling duration investigated in this work (i.e., 40 min) resulted in 95% of the fibres having a length $< 5 \mu\text{m}$ (Figure 6).

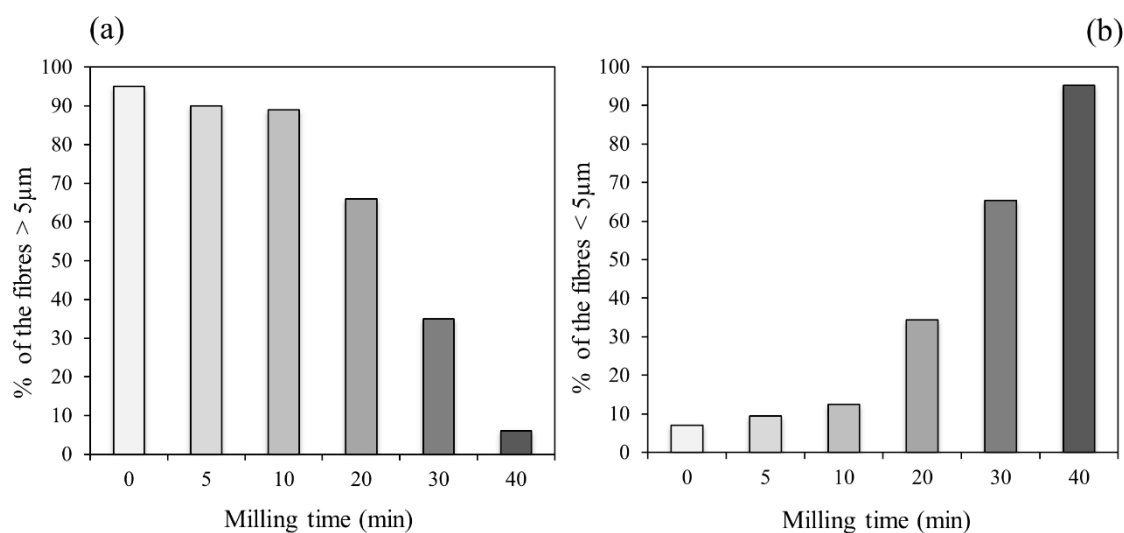


Figure 6. Percentage of long ($L > 5 \mu\text{m}$) and short ($L < 5 \mu\text{m}$) chrysotile fibres vs. milling time (from 0 to 40 min). (a) Chrysotile fibre length fraction $> 5 \mu\text{m}$. (b) Chrysotile fibre length fraction $< 5 \mu\text{m}$.

XRPD data (Figure 3) and FTIR spectra (Figure 5) did not evidence any structural changes imposed by milling, as the data remained substantially invariant. Instead, the contrary was observed in earlier studies dealing with traditional milling methods. For example, Suquet [31] studied the effect of dry milling on the crystal structure of chrysotile. The author observed important changes in the diffraction pattern following milling in terms of intensity loss and peak broadening [31]. IR analyses showed that dry milling led to important changes in the lattice vibrations, indicating a disrupted chrysotile structure and the formation of amorphous silica [31]. The IR data indicated the presence of adsorbed CO_2 and H_2O on the surface of milled chrysotile, which, according to the author, was explained by newly formed reactive surface sites [31]. Iwaszko et al. [30] performed an FTIR investigation of asbestos–cement containing chrysotile before and after prolonged high-energy ball milling. In particular, changes in the intensity and position of the chrysotile bands provoked by milling were evaluated. The authors observed a gradual disappearance of the characteristic bands as the milling time increased, being virtually extinct following 3 h of ball milling [30]. Bloise et al. [37] conducted dry milling of chrysotile using a ring and puck mill and the XRPD data showed a continuous amorphization of the fibres, which, following 10 min of mechanical action, was near complete.

The temperature during milling is a key factor determining the different outcome obtained by cryo-milling in comparison to traditional milling. Lowering the temperature to cryogenic conditions changes the mechanical behaviour of the material from ductile to brittle. Hence, the stress imposed by the milling medium results in brittle fracture rather than structural changes. In addition, temperature-induced dehydroxylation of chrysotile observed during traditional milling is avoided [37]. Even though the macroscopic temperature of the system generally is moderate, the local microscopic temperature can be even higher than $1000 \text{ }^\circ\text{C}$ [53]. The reaction mechanism by which chrysotile transforms into an amorphous phase following temperature-induced dehydroxylation has been elucidated in previous work [54]. The rate-limiting step of the reaction was found to be one-dimensional

diffusion with an instantaneous or decelerator rate of nucleation [54]. This result was explained by the peculiar structure of chrysotile: this mineral is a hydrated magnesium silicate with the ideal chemical formula $Mg_3(OH)_4Si_2O_5$. The double-layered structure is composed of an octahedral $Mg(OH)_2$ sheet (O) bonded to a tetrahedral SiO_2 (T) sheet, with the Mg cations fully occupying the octahedral cation sites. The fibrous nature of chrysotile is due to a lattice misfit between the two layers, giving rise to a strain gradient that leads to self-rolling and the formation of a fibre structures with the $Mg(OH)_2$ surface exposed externally. Cattaneo et al. [54] concluded that the most probable one-dimensional escape paths for the water molecules were along the fibre axis. In this work, the FTIR analyses suggested that this process does not occur during cryogenic milling (Figure 5). As shown in Figure 5b, the FTIR spectrum of chrysotile milled for 40 min preserved the characteristic bands assigned to the OH groups (i.e., 3643 and 3682 cm^{-1}).

In the literature, various methodologies have been proposed to produce size-selected fibre samples as discussed in the introduction. Two-step procedures are generally applied, including comminution followed by size separation. Currently, gravitational wet separation of hand-milled fibres is the most common method of obtaining groups of fibres differing in length. This process is relatively time-consuming due to slow settling velocity (ca. 3 h for asbestos fibres according to [55]) and the fact that the solvent must be evaporated from the sorted fibres prior to use.

The results shown in this work evidenced that the two desired size classes for *in vitro* toxicology studies (i.e., $L < 5\mu m$ and $L > 5\mu m$), could be directly obtained by cryo-milling without a subsequent separation step [25]. In fact, milling for 40 min directly delivered a batch consisting only of short fibres (95% $< 5\mu m$), whereas 10 min of cryo-milling resulted in a batch containing mainly long fibres (mean $L = 14.32\mu m$ and 90% of fibres with $L > 5\mu m$). These two sets of fibres are suitable as they are, without the need for an additional size separation step. Another important advantage of the cryo-milled fibres (especially considering the upper length size class) was that stable fibre suspensions, ready to be added to the culture media for *in vitro* testing, could easily be prepared by ultrasonification of the cryo-milled fibres in a biological solution. In fact, even though most of the fibres were still arranged in bundles following mechanical pre-treatment under cryogenic conditions, they were easy to split by ultrasonic treatment. This was shown to be difficult to achieve with the very long and curly pristine fibres that, instead, tended to agglomerate in large clusters (not shown here).

5. Conclusions

In this work, cryogenic milling was systematically explored as a comminution method of a commercial Russian chrysotile. The high potential of this route is due to the embrittlement of the material, which facilitates brittle fracture and thus size reduction without plastic deformation.

The aim was to prepare different length classes of fibres suitable for *in vitro* studies, i.e., $<5\mu m$ and $>5\mu m$, without modifying the crystal–chemical properties of the original ones. This particular mineral is currently used in pro-chrysotile countries and studies aimed at shedding light on their potential health hazards are highly motivated.

Analyses of SEM images showed a successive length reduction when the duration of cryo-milling increased from 5 to 40 min (the investigated time range). XRPD and FTIR data collected from these samples did not evidence any changes in crystallinity or microstructure.

It was shown that the two desired size classes of fibres could be obtained by modifying the milling duration: the class of long fibres was obtained following 10 min of milling (i.e., 90% $> 5\mu m$), whereas the class of short ones could be prepared by prolonging the milling time to 40 min (i.e., 95% $> 5\mu m$).

Stable fibre suspensions, ready to be added to the culture media for *in vitro* testing, could be easily obtained by ultrasonification of the cryo-milled fibres in a biological solution in which the bundles were easily split. Compared to the most common method for

the preparation of different size classes of fibres, i.e., gentle hand milling followed by gravitational separation, cryo-milling allows a rapid preparation of the two desired size classes without the need of further separation.

Author Contributions: Conceptualization, A.F.G., D.D.G. and V.S.; methodology, A.F.G., D.D.G. and V.S.; validation, A.F.G., M.L.G. and L.T.; formal analysis, V.S. and D.D.G.; investigation, V.S. and D.D.G.; resources, A.F.G.; data curation, V.S., D.D.G. and A.F.G.; writing—original draft preparation, V.S., D.D.G., A.F.G. and M.L.G.; writing—review and editing, V.S., D.D.G., A.F.G., M.L.G. and L.T.; project administration, A.F.G.; funding acquisition, A.F.G. All authors have read and agreed to the published version of the manuscript.

Funding: This research was conducted under the project “Fibres a Multidisciplinary Mineralogical, Crystal-Chemical and Biological Project to Amend the Paradigm of Toxicity and Cancerogenicity of Mineral Fibres” (PRIN: PROGETTI DI RICERCA DI RILEVANTE INTERESSE NAZIONALE–Bando 2017-Prot. 20173X8WA4). The study was further supported in part by the project “CCIAARE–Attuazione di un progetto di accompagnamento delle imprese nell’ambito del progetto PID impresa 4.0” financed by the Camera di Commercio di Reggio Emilia (Italy).

Institutional Review Board Statement: Not applicable.

Informed Consent Statement: Not applicable.

Data Availability Statement: Not applicable.

Conflicts of Interest: The authors declare no conflict of interest.

References

1. Ross, M.; Nolan, R.P. History of asbestos discovery and use and asbestos-related disease in context with the occurrence of asbestos within ophiolite complexes. In *Ophiolite Concept and the Evolution of Geological Thought*; Dilek, Y., Newcomb, S., Eds.; Geological Society of America: Boulder, CO, USA, 2003; pp. 447–470.
2. NIOSH. *Asbestos Fibers and Other Elongate Mineral Particles: State of the Science and Roadmap for Research*; National Institute for Occupational Safety and Health: Cincinnati, OH, USA, 2011; pp. 1–153.
3. IARC. Asbestos (chrysotile, amosite, crocidolite, tremolite, actinolite, and anthophyllite). *IARC Monogr.* **2012**, *100*, 219–309.
4. WHO. *Outline for the Development of National Programmes for Elimination of Asbestos-Related Diseases*; World Health Organization: Geneva, Switzerland, 2007; pp. 1–20.
5. Carbone, M.; Adusumilli, P.S.; Alexander, H.R., Jr.; Baas, P.; Bardelli, F.; Bononi, A.; Bueno, R.; Felley-Bosco, E.; Galateu-Salle, F.; Jablons, D.; et al. Mesothelioma: Scientific clues for prevention, diagnosis, and therapy. *CA Cancer. J. Clin.* **2019**, *69*, 402–429. [[CrossRef](#)]
6. Cavone, D.; Caputi, A.; De Maria, L.; Cannone, E.S.S.; Mansi, F.; Birtolo, F.; Delfino, C.M.; Vimercati, L. Epidemiology of Mesothelioma. *Environments* **2019**, *6*, 76. [[CrossRef](#)]
7. Pass, H.I.; Alimi, M.; Carbone, M.; Yang, H.; Goparaju, C.M. Mesothelioma Biomarkers: Discovery in Search of Validation. *Thorac. Surg. Clin.* **2020**, *30*, 395–423. [[CrossRef](#)] [[PubMed](#)]
8. Donaldson, K.; Murphy, F.A.; Duffin, R.; Poland, C.A. Asbestos, carbon nanotubes and the pleural mesothelium: A review of the hypothesis regarding the role of long fibre retention in the parietal pleura, inflammation and mesothelioma. *Part Fibre Toxicol.* **2010**, *7*, 5. [[CrossRef](#)]
9. Gualtieri, A.F.; Mossman, B.T.; Roggli, V.L. Towards a general model for predicting the toxicity and pathogenicity of minerals fibres. In *Mineral Fibres: Crystal Chemistry, Chemical-Physical Properties, Biological Interaction and Toxicity*; Gualtieri, A.F., Ed.; European Mineralogical Union: London, UK, 2017; pp. 501–526.
10. Mossman, B.T.; Gualtieri, A.F. Lung Cancer: Mechanisms of Carcinogenesis by Asbestos. In *Occupational Cancers*; Anttila, S., Boffetta, P., Eds.; Springer: Berlin/Heidelberg, Germany, 2020; pp. 239–256.
11. Gualtieri, A.F.; Lusvardi, G.; Zoboli, A.; Di Giuseppe, D.; Lassinantti Gualtieri, M. Biodurability and release of metals during the dissolution of chrysotile, crocidolite and fibrous erionite. *Environ. Res.* **2019**, *171*, 550–557. [[CrossRef](#)] [[PubMed](#)]
12. Di Giuseppe, D.; Zoboli, A.; Vigliaturo, R.; Gieré, R.; Bonasoni, M.P.; Sala, O.; Gualtieri, A.F. Mineral fibres and asbestos bodies in human lung tissue: A case study. *Minerals* **2019**, *9*, 618. [[CrossRef](#)]
13. Giacobbe, C.; Di Giuseppe, D.; Zoboli, A.; Lassinantti Gualtieri, M.; Bonasoni, P.; Moliterni, A.; Corriero, N.; Altomare, A.; Wright, J.; Gualtieri, A.F. Crystal structure determination of a lifelong biopersistent asbestos fibre using single-crystal synchrotron X-ray micro-diffraction. *IUCrJ* **2021**, *8*, 76–86. [[CrossRef](#)] [[PubMed](#)]
14. Yarborough, C.M. Chrysotile as a cause of mesothelioma: An assessment based on epidemiology. *Crit. Rev. Toxicol.* **2006**, *36*, 165–187. [[CrossRef](#)] [[PubMed](#)]
15. Pira, E.; Romano, C.; Donato, F.; Pelucchi, C.; La Vecchia, C.; Boffetta, P. Mortality from cancer and other causes among Italian chrysotile asbestos miners. *Occup. Environ. Med.* **2017**, *74*, 558–563. [[CrossRef](#)]

16. Kanarek, M.S. Mesothelioma from chrysotile asbestos: Update. *Ann. Epidemiol.* **2011**, *21*, 688–697. [CrossRef]
17. Gilham, C.; Rake, C.; Burdett, G.; Nicholson, A.G.; Davison, L.; Franchini, A.; Carpentre, J.; Hodgson, J.; Darnton, A.; Peto, J. Pleural mesothelioma and lung cancer risks in relation to occupational history and asbestos lung burden. *Occup. Environ. Med.* **2016**, *73*, 290–299. [CrossRef] [PubMed]
18. Yao, S.; Iezzi, G.; Della Ventura, G.; Bellatreccia, F.; Petibois, C.; Marcelli, A.; Nazzari, M.; Lazzarin, F.; Di Gioacchino, M.; Petrarca, C. Mineralogy and textures of riebeckitic asbestos (crocidolite): The role of single versus agglomerated fibres in toxicological experiments. *J. Hazard. Mater.* **2017**, *340*, 472–485. [CrossRef] [PubMed]
19. Current Asbestos Bans. International Ban Asbestos. Secretariat. Available online: http://www.ibasecretariat.org/alpha_ban_list.php (accessed on 13 April 2021).
20. Asbestos Statistics and Information. United States Geological Service. Available online: <https://pubs.usgs.gov/periodicals/mcs2020/mcs2020-asbestos.pdf> (accessed on 6 January 2021).
21. Di Giuseppe, D.; Zoboli, A.; Nodari, L.; Pasquali, L.; Sala, O.; Ballirano, P.; Malferrari, D.; Raneri, S.; Hanuskova, M.; Gualtieri, A.F. Characterization and assessment of the potential toxicity/pathogenicity of Russian commercial chrysotile. *Am. Min.* **2021**. [CrossRef]
22. Ferrante, D.; Mirabelli, D.; Silvestri, S.; Azzolina, D.; Giovannini, A.; Tribaudino, P.; Magnani, C. Mortality and mesothelioma incidence among chrysotile asbestos miners in Balangero, Italy: A cohort study. *Am. J. Ind. Med.* **2020**, *63*, 135–145. [CrossRef]
23. Pollastri, S.; Perchiazzi, N.; Lezzerini, M.; Plaisier, J.R.; Cavallo, A.; Dalconi, M.C.; Bursi Gandolfi, N.; Gualtieri, A.F. The crystal structure of mineral fibres. 1. Chrysotile. *Period. Miner.* **2016**, *85*, 249–259.
24. Spurny, K.R.; Stöber, W.; Opiela, H.; Weiss, G. Size-selective preparation of inorganic fibers for biological experiments. *Am. Ind. Hyg. Assoc. J.* **1979**, *40*, 20–38. [CrossRef] [PubMed]
25. Myojo, T.; Kohyama, N. Separation of Asbestos Fibers by Length—Procedure for Obtaining Different-length Samples for Biological Experiments. *J. Soc. Powder Technol. Jpn.* **1992**, *27*, 804–810. [CrossRef]
26. Vigliaturo, R.; Choi, J.K.; Pérez-Rodríguez, I.; Gieré, R. Dimensional distribution control of elongated mineral particles for their use in biological assays. *MethodsX* **2020**, *28*, 100937. [CrossRef] [PubMed]
27. Jolicoeur, C.; Roberge, P.; Fortier, J.L. Separation of short fibres from bulk chrysotile asbestos fiber materials: Analysis and physico-chemical characterization. *Can. J. Chem.* **1981**, *59*, 1140–1148. [CrossRef]
28. Turci, F.; Tomatis, M.; Pacella, A. Surface and bulk properties of mineral fibres relevant to toxicity. In *Mineral Fibres: Crystal Chemistry, Chemical-Physical Properties, Biological Interaction and Toxicity*; Gualtieri, A.F., Ed.; European Mineralogical Union: London, UK, 2017; pp. 171–214.
29. Assuncao, J.; Corn, M. The effects of milling on diameters and lengths of fibrous glass and chrysotile asbestos fibers. *Am. Ind. Hyg. Assoc. J.* **1975**, *36*, 811–819. [CrossRef] [PubMed]
30. Iwaszko, J.; Zawada, A.; Lubas, M. Influence of high-energy milling on structure and microstructure of asbestos-cement materials. *J. Mol. Struct.* **2018**, *1155*, 51–57. [CrossRef]
31. Suquet, H. Effects of dry grinding and leaching on the crystal structure of chrysotile. *Clays Clay Miner.* **1989**, *37*, 439–445. [CrossRef]
32. Occella, E. Analysis of asbestos in bulk materials by X-ray diffraction: Influence of grinding methods on the result. *KONA Powder Part. J.* **1994**, *12*, 43–52. [CrossRef]
33. Spurny, K.R.; Stöber, W.; Opiela, H.; Weiss, G. On the problem of milling and ultrasonic treatment of asbestos and glass fibers in biological and analytical applications. *Am. Ind. Hyg. Assoc. J.* **1980**, *41*, 198–203. [CrossRef]
34. Papirer, E.; Roland, P. Grinding of chrysotile in hydrocarbons, alcohol, and water. *Clays Clay Miner.* **1981**, *29*, 161–170. [CrossRef]
35. Salamati-pour, A.; Mohanty, S.K.; Pietrofesa, R.A.; Vann, D.R.; Christofidou-Solomidou, M.; Willenbring, J.K. Asbestos fiber preparation methods affect fiber toxicity. *Environ. Sci. Technol. Lett.* **2016**, *3*, 270–274. [CrossRef]
36. Plescia, P.; Gizzi, D.; Benedetti, S.; Camilucci, L.; Fanizza, C.; De Simone, P.; Paglietti, F. Mechanochemical treatment to recycling asbestos-containing waste. *Waste Manag.* **2003**, *23*, 209–218. [CrossRef]
37. Bloise, A.; Catalano, M.; Gualtieri, A.F. Effect of milling on chrysotile, amosite and crocidolite and implications for thermal treatment. *Minerals* **2018**, *8*, 135. [CrossRef]
38. Turci, F.; Colonna, M.; Tomatis, M.; Mantegna, S.; Cravotto, G.; Gulino, G.; Aldieri, E.; Ghigo, D.; Fubini, B. Surface reactivity and cell responses to chrysotile asbestos nanofibers. *Chem. Res. Toxicol.* **2012**, *25*, 884–894. [CrossRef]
39. Thorne, P.S.; Lightfoot, E.N.; Albrecht, R.M. Physicochemical characterization of cryogenically ground, size separated, fibrogenic particles. *Environ. Res.* **1985**, *36*, 89–110. [CrossRef]
40. Sailors, R.; Corten, H. Relationship between Material Fracture Toughness using Fracture Mechanics and Transition Temperature Tests. In *Fracture Toughness, Part II*; Corten, H., Ed.; ASTM International: West Conshohocken, PA, USA, 1972; pp. 164–191.
41. Paul, S.; Chattopadhyay, A.B. The effect of cryogenic cooling on grinding forces. *Int. J. Mach. Tool Manuf.* **1996**, *36*, 63–72. [CrossRef]
42. Kumar, N.; Biswas, K. Cryomilling: An environment friendly approach of preparation large quantity ultrafine pure aluminium nanoparticles. *J. Mater. Res. Technol.* **2019**, *8*, 63–74. [CrossRef]
43. Zoboli, A.; Di Giuseppe, D.; Baraldi, C.; Gamberini, M.C.; Malferrari, D.; Urso, G.; Lassinantti Gualtieri, M.; Bailey, M.; Gualtieri, A.F. Characterisation of fibrous ferrierite in the rhyolitic tuffs at Lovelock, Nevada, USA. *Miner. Mag.* **2019**, *83*, 577–586. [CrossRef]
44. Image]. Available online: <https://imagej.nih.gov/ij> (accessed on 13 April 2021).

45. Degen, T.; Sadki, M.; Bron, E.; König, U.; Nénert, G. The HighScore Suite. *Powder Diffr.* **2014**, *29*, 13–18. [[CrossRef](#)]
46. Ferreira, I.C.; Aguiar, E.M.; Silva, A.T.; Santos, L.L.; Cardoso-Sousa, L.; Araújo, T.G.; Santos, D.W.; Goulart, L.R.; Sabino-Silva, R.; Maia, Y.C. Attenuated Total Reflection-Fourier Transform Infrared (ATR-FTIR) Spectroscopy Analysis of Saliva for Breast Cancer Diagnosis. *J. Oncol.* **2020**, *2020*, 4343590. [[CrossRef](#)]
47. Di Giuseppe, D.; Perchiazzi, N.; Brunelli, D.; Giovanardi, T.; Nodari, L.; Della Ventura, G.; Malferrari, D.; Maia, M.; Gualtieri, A.F. Occurrence and characterization of tremolite asbestos from the Mid Atlantic Ridge. *Sci. Rep.* **2021**, *11*, 6285. [[CrossRef](#)]
48. Della Ventura, G. The analysis of asbestos minerals using vibrational spectroscopies (FTIR, Raman): Crystal-chemistry, identification and environmental applications. In *Mineral Fibres: Crystal Chemistry, Chemical-Physical Properties, Biological Interaction and Toxicity*; Gualtieri, A.F., Ed.; European Mineralogical Union: London, UK, 2017.
49. Hofmeister, A.M.; Bowey, J.E. Quantitative infrared spectra of hydrosilicates and related minerals. *Mon. Not. R. Astron. Soc.* **2006**, *367*, 577–591. [[CrossRef](#)]
50. Rivero Crespo, M.A.; Pereira Gómez, D.; Villa Garcí, M.V.; Gallardo Amores, J.M.; Sánchez Escribano, V. Characterization of serpentines from different regions by transmission electron microscopy, X-ray diffraction, BET specific surface area and vibrational and electronic spectroscopy. *Fibers* **2019**, *7*, 47. [[CrossRef](#)]
51. Giacobbe, C.; Gualtieri, A.F.; Quartieri, S.; Rinaudo, C.; Allegrin, M.; Andreozzi, G.B. Spectroscopic study of the product of thermal transformation of chrysotile-asbestos containing materials (ACM). *Eur. J. Miner.* **2010**, *22*, 535–546. [[CrossRef](#)]
52. Sedman, J.; van de Voort, F.R.; Ismail, A.A. Attenuated total reflectance spectroscopy: Principles and applications in Infrared analysis of food. In *Spectral Methods in Food Analysis*; Mossoba, M.M., Ed.; Marcel Dekker Inc.: New York, NY, USA, 1999; pp. 397–426.
53. Suryanarayana, C. Mechanical alloying and milling. *Prog. Mater. Sci.* **2001**, *46*, 1–184. [[CrossRef](#)]
54. Cattaneo, A.; Gualtieri, A.F.; Artioli, G. Kinetic study of the dehydroxylation of chrysotile asbestos with temperature by in situ XRPD. *Phys. Chem. Miner.* **2003**, *30*, 177–183. [[CrossRef](#)]
55. Pollastri, S.; Gualtieri, A.F.; Lassinantti Gualtieri, M.; Hanuskova, M.; Cavallo, A.; Gaudino, G. The zeta potential of mineral fibres. *J. Hazard. Mater.* **2014**, *276*, 469–479. [[CrossRef](#)]